

PROPERTIES OF HEAVY AND SUPERHEAVY NUCLEI

A. Sobiczewski

Soltan Institute for Nuclear Studies, Warsaw, Poland

Recent studies of the properties of heaviest nuclei done in our theoretical group in Warsaw are shortly reviewed. They concentrate mainly on two topics: heights of static fission barriers B_f^{st} and single-particle properties of these nuclei. In the analysis of B_f^{st} , a crucial role is played by the deformation space used in the analysis. Results obtained in the case when only axially symmetric shapes of a nucleus are admitted, and also when non-axial deformations are included, are illustrated. Concerning the single-particle properties of heaviest nuclei, one-quasiparticle spectra of them are discussed. Influence of the spectra on the transition energies in the α -decay chains and also on the α -decay half-lives are illustrated.

1. Introduction

There is a fast progress in the studies of heavy and superheavy nuclei in recent years. This concerns both the experimental research (e.g., [1 - 5]) and the theoretical one (e.g., [6 - 10]). Also chemical investigations on superheavy elements (SHE) contribute very importantly to this development (e.g., [11 - 16]), as they need the synthesis of superheavy nuclei (SHN), which is done by physical methods and supplies us with a knowledge on the process of this synthesis and also on the properties of SHN, in particular on their decay.

By superheavy nuclei, one presently understands nuclei which exist due to their shell structure [17, 18]. As description of shell structure and effects of this structure on half-lives of nuclei depends on the approach used, this definition is not sharp. All realistic descriptions, however, indicate that these are roughly the nuclei with atomic number $Z \geq 104$, i.e., nuclei of transactinide elements.

If one adopts this definition, synthesis of about 85 SHN with $Z=104 - 118$ (except $Z=117$), i.e., of 14 SHE has been already reported. Half of these elements have already names accepted by the International Union of Pure and Applied Chemistry (IUPAC).

Small cross sections for synthesis of SHN (generally below nanobarns) and, simultaneously, short half-lives (generally below seconds) is the reason that these nuclei cannot be cumulated. Before synthesis of a next nucleus, the previous one is already decayed. This results then in a specific property of physics of SHN and chemistry of SHE. This is physics of single nuclei and chemistry of single atoms. All the studies are done on the scale of one nucleus or one atom at a time. Corresponding to this, specific methods, physical and chemical, of the investigation of these nuclei and elements had to be, and have been, developed.

The objective of this paper is to give a short review of recent studies done in our theoretical group in Warsaw. The studies concentrated mainly on the analysis of the height of the static fission barriers B_f^{st} of heaviest nuclei and on the single-particle properties of them.

A study of the barrier height B_f^{st} of heaviest nuclei is motivated by the importance of this quantity in calculations of cross sections σ for the synthesis of them (e.g., [19, 20]). This height is a decisive quantity in the competition between neutron evaporation and fission of a compound nucleus in the process of its cooling. A large sensitivity of σ to B_f^{st} stresses a need for accurate calculations of B_f^{st} . For example, a change of B_f^{st} by 1 MeV may result in a change of σ by about one order of magnitude or even more [21]. The basic role in the calculations of B_f^{st} is played by the deformation space admitted in them. Up to the present, the height B_f^{st} has been mostly studied in the case of axial symmetry of a nucleus (e.g., [22 - 25]). Studies taking into account non-axial degrees of freedom were more seldom. Results obtained in both cases will be illustrated in the present paper.

A need for studies of single-particle properties of heaviest nuclei is stressed by the fact that most of our knowledge of these nuclei comes from the observation of α -decay chains of odd-A and odd-odd nuclei. Theoretical analysis of such chains requires the knowledge of single-particle spectra of these nuclei. Examples of such an analysis is given in the article.

2. Theoretical model

The calculations are done within a macroscopic-microscopic approach. The Yukawa-plus-exponential model [26] is used for the calculation of the macroscopic part of energy of a nucleus, and the Strutinski shell

correction [27] is taken for its microscopic part. The Woods - Saxon single-particle potential, with the "universal" variant of its parameters found in [28] and also specified explicitly in [29], is used for description of the single-particle properties of a nucleus. Values of parameters of the macroscopic part of mass are taken the same as in [30], where they were adjusted to experimental masses [31] of even-even heaviest nuclei with atomic number $Z \geq 84$.

A large, 7-dimensional deformation space, $\{\beta_\lambda\}$, $\lambda = 2, 3, \dots, 8$, is used to obtain the equilibrium deformation of a nucleus. The contribution of an odd nucleon, occupying a single-particle state $|\mu\rangle$, to energy of a nucleus is described by the one-quasiparticle energy $E_\mu = \sqrt{(e_\mu - \lambda)^2 + \Delta^2}$. Here, e_μ is the energy of the odd nucleon in the state $|\mu\rangle$ and Δ is the pairing-energy gap parameter, calculated in the BCS approximation. Pairing interaction of the monopole type, with the same strength parameters as in [30], is taken. No blocking is used. The calculations are done in a similar way to that of [32, 33].

3. Fission barriers

As already stated in the Introduction, a basic role in the calculated value of the height of the static fission barrier B_f^{st} is played by the deformation space which is used in the calculation. In the present section, we will illustrate this for both cases of a deformed and a spherical nucleus.

We start from the case of axial symmetry of nuclear shapes, the case in which most of the calculations have been done.

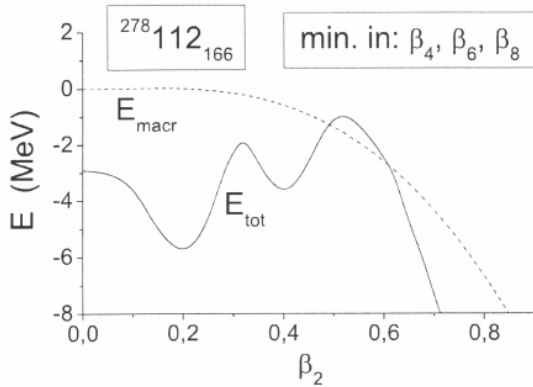


Fig. 1. Static spontaneous-fission barrier calculated for the nucleus $^{278}_{112}_{166}$ in two cases, when only the macroscopic (E_{macr}) and when the total (E_{tot}) energy of it is considered [34].

Fig. 1, taken from [34], shows an example of the ground-state static fission barrier of the superheavy nucleus $^{278}_{112}$. One can see that a rather high barrier is obtained for this very heavy nucleus, which is entirely created by effects of shell structure in energy of this nucleus. Without this structure (see macroscopic part of the energy, E_{macr}), no barrier is obtained. The largest shell correction to the macroscopic part of the energy is obtained at the (deformed) equilibrium point (about 6 MeV), smaller (about 1.8 MeV) at the first, and the smallest (about 0.5 MeV) at the second saddle point. Significant shell corrections at the saddle points are worth to be noticed as these corrections are quite often neglected in various estimates of the static fission barriers of superheavy nuclei. In the figure, the dependence of energy of the nucleus on deformation β_2 is plotted.

However, at each value of β_2 , the energy is minimized in the β_4 , β_6 and β_8 degrees of freedom. Here, β_λ , $\lambda = 2, 4, 6, 8$, are the usual deformation parameters, appearing in the expression for nuclear radius (in the intrinsic frame of reference) in terms of spherical harmonics $Y_{\lambda 0}(\mathcal{G})$,

$$R(\mathcal{G}) = R_0(\beta_\mu) \left[1 + \sum_{\lambda} \beta_\lambda Y_{\lambda 0}(\mathcal{G}) \right], \quad (1)$$

where the dependence of R_0 on β_μ is determined by the volume-conservation condition.

Fig. 2 [35, 36] (cf. also [37]) illustrates the role of the dimension of the deformation space, in which B_f^{st} is analyzed, for a deformed nucleus (^{250}Cf) and a spherical one ($^{294}_{116}$). In the figure, the energy of a nucleus at its minimum, E_{min} , at its saddle point, E_s , and the barrier height, $B_f^{\text{st}} = E_s - (E_{\text{min}} + E_{\text{zp}})$, is calculated in 1-, 2-, 3- and 4-dimensional deformation spaces. Here, E_{zp} is the zero-point energy in the fission degree of freedom, which is taken $E_{\text{zp}} = 0.7$ MeV for all analyzed nuclei (see [18, 29]). As only even-multipolarity deformations (to describe thin barriers of very heavy nuclei) are taken, this is the calculation of B_f^{st} as a

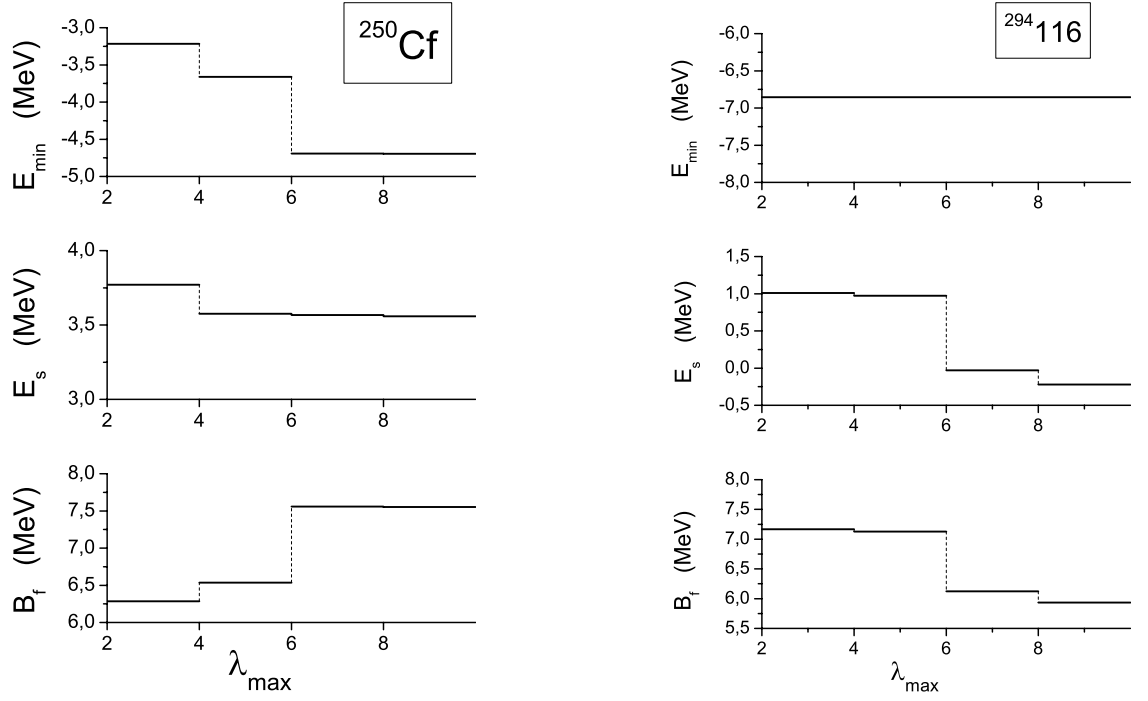


Fig. 2. Dependence of the potential energy of the nucleus ^{250}Cf (l.h.s.) and $^{294}116$ (r.h.s.) at the equilibrium, E_{\min} , and at the saddle point, E_s , and also of the barrier height, B_f^{st} , on the maximal multipolarity λ_{\max} of the deformation taken in the analysis [35, 36].

function of the maximal multipolarity $\lambda_{\max} = 2, 4, 6$ and 8 . The figure shows the dependence of E_{\min} , E_s and B_f^{st} on λ_{\max} . One can see in the left part of the figure [35] that for the deformed nucleus, ^{250}Cf , E_{\min} decreases more strongly than E_s when λ_{\max} is increasing, resulting in the increase of B_f^{st} with increasing λ_{\max} . A rather important role of β_6 in E_{\min} (and thus in B_f^{st}) is seen, while almost no effect of β_8 is observed, for the analyzed nucleus ^{250}Cf .

For the nucleus $^{294}116$ [36], due to its spherical shape at the equilibrium (E_{\min} is independent of λ_{\max}), the barrier B_f^{st} decreases with increasing λ_{\max} just in the same way as does E_s . It is worthy to be aware of this difference in the role of the dimension of the deformation space, between a deformed and a spherical nucleus.

Values of B_f^{st} calculated by a macro-micro method for many superheavy nuclei with $Z=106-120$ have been presented in [23]. Axial symmetry of the nuclei has been assumed in the calculations.

Influence of non-axial shapes of a nucleus on the barrier height B_f^{st} is illustrated in Fig. 3 [35] for ^{250}Cf . Here, the 5-dimensional deformation space is used. It is specified by the following expression for the nuclear radius $R(\vartheta, \varphi)$ (taken in the intrinsic frame of reference) in terms of spherical harmonics $Y_{\lambda\mu}$

$$R(\vartheta, \varphi) = R_0 \left\{ 1 + \beta_2 [\cos \gamma Y_{20} + \frac{1}{\sqrt{2}} \sin \gamma Y_{22}] + \beta_4 Y_{40} + \beta_6 Y_{60} + \beta_8 Y_{80} \right\}, \quad (2)$$

where $\gamma \equiv \gamma_2$ is the Bohr quadrupole non-axiality parameter and the dependence of R_0 on the deformation parameters is determined by the volume-conservation condition. In the figure, the potential energy, minimized in $\beta_4, \beta_6, \beta_8$, is projected on the plane $(\beta_2 \cos \gamma, \beta_2 \sin \gamma)$. One can see that the inclusion of non-axial shapes decreases the potential energy at the saddle point by 1.7 MeV. As non-axial shapes do not decrease the potential energy at the equilibrium point, they decrease the barrier height B_f^{st} by the same amount of 1.7 MeV. Only after the inclusion of this decrease, the calculated barrier height $B_f^{\text{st}} = 7.5 - 1.7 = 5.8$ MeV, becomes close to measured value (5.6 ± 0.3) MeV [38]. The mechanism by which the quadrupole non-axiality decreases the barrier height B_f^{st} has been studied in [39].

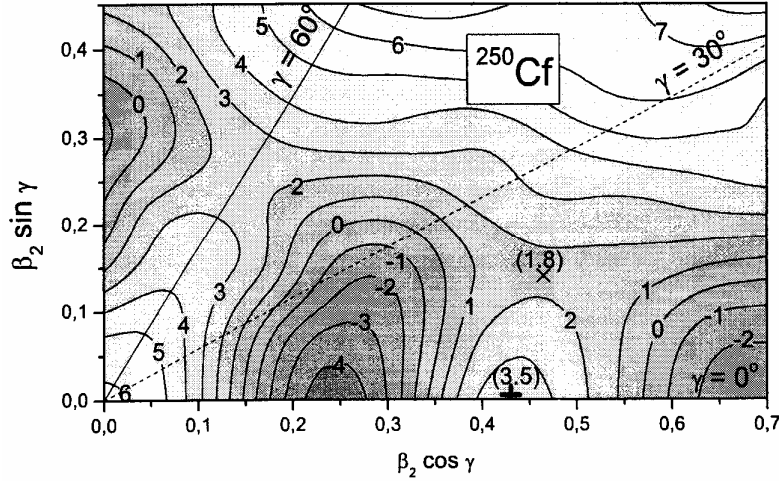


Fig. 3. Contour map of the potential energy of the nucleus ^{250}Cf in the case when non-axial shapes are taken into account. The position of the saddle point is marked by the symbol "+", when axial symmetry of the nucleus is assumed, and by the symbol "x", when non-axiality is taken into account. Numbers in parentheses specify the values of the energy at these points [35].

4. Single-particle properties

Let us illustrate first the quality of the description of single-particle excitation energies, obtained within the model used by us.

Fig. 4 [40] shows a comparison between theoretical and experimental excitation energies of proton single-particle states obtained for the nucleus ^{241}Am . (In this figure, similar to a number of other figures in this article, we give the spin projection Ω of a state on the symmetry axis multiplied by 2: 2Ω instead of Ω , for simplicity of notation). Theoretical excitation energies are obtained in the one-quasiparticle approximation, i.e., as $E_\mu = \sqrt{(e_\mu - \lambda)^2 + \Delta^2}$, where e_μ is the energy of the odd nucleon in the state $|\mu\rangle$, λ is the Fermi energy, and Δ is the pairing-energy gap parameter, calculated in the BCS approach. One can see that the observed ground state is reproduced by the calculations. Also the sequence in energy of the observed states is reproduced. Average of absolute values of the discrepancies $\delta E_\mu \equiv E_\mu^{\text{th}} - E_\mu^{\text{exp}}$ for 4 observed excited states is 108 keV and rms of these values is 150 keV. Difference between the average and rms values of $|\delta E_\mu|$ characterizes the non-uniformity of the distribution of these quantities. One can see in Fig. 4 that this non-uniformity is rather large.

As already stated in Sect. 2, the theoretical spectrum of Fig. 4 has been obtained with the use of a large, 7-dimensional deformation space $\{\beta_\lambda\}$, $\lambda = 2, 3, \dots, 8$. This is because of a need for accurate determination of the equilibrium deformation of a nucleus, to which the calculated excitation energies E_μ are sensitive. Fig. 5 illustrates the sensitivity of the calculated spectrum of the nucleus ^{241}Am to changes of the main (quadrupole) component of the deformation around its equilibrium value. One can see that a change of β_2 by a rather small value $\Delta\beta_2 = 0.02$ may result in a quite large change of the excitation energy of a state by about 300 keV. As a rule, changes of the excitation energy of low states are smaller than those of higher ones.

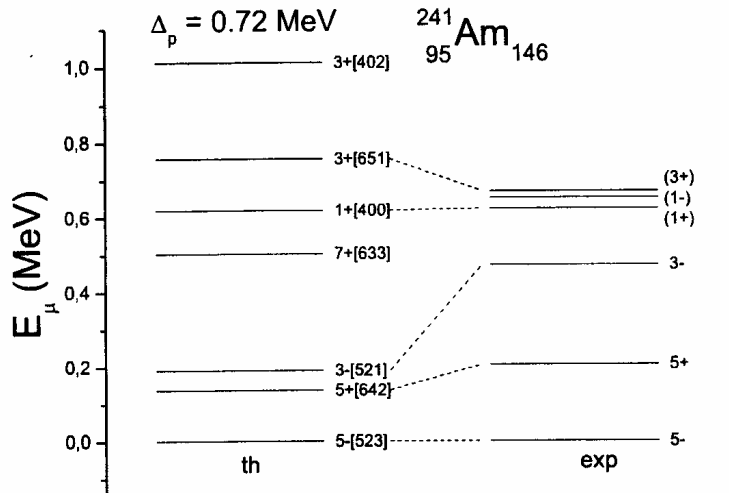


Fig. 4. Comparison between theoretical and experimental excitation energies of proton single-particle states of the nucleus ^{241}Am . The calculated proton pairing-energy gap parameter Δ_p is also given. Quantum numbers 2Ω and π are given at each energy level and the usual Nilsson labels $[Nn_z\Lambda]$ are also shown at each calculated level [40].

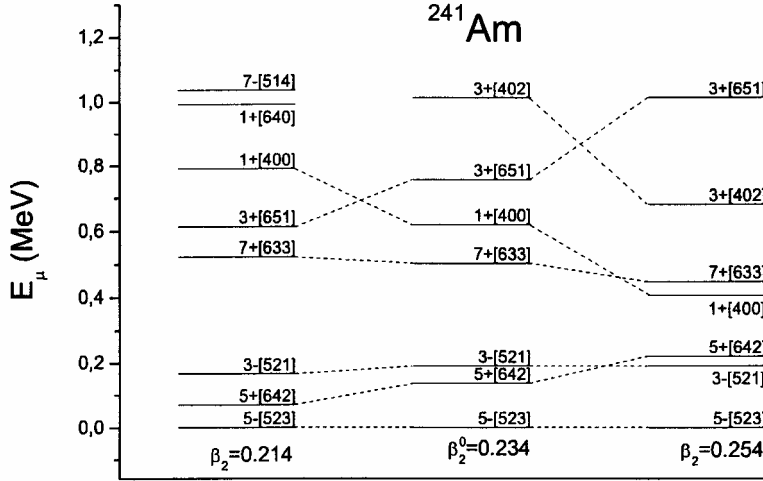


Fig. 5. Sensitivity of single-proton spectrum of ^{241}Am to changes of the quadrupole deformation β_2 [41].

Finally, Fig. 6 [42] shows a theoretical interpretation of the experimentally known [43, 44] α -decay chain of the nucleus ^{271}Ds ($Z = 110$). Such an interpretation helps to draw important knowledge on the structure of nuclei, appearing in the chain, from experimental data. A general assumption is that the α transitions occur between the states with the same structure (the same quantum numbers). If a transition to an excited state takes place, the most probable γ decay to a lower state is assumed to occur before the next α transition. Even with these assumptions, however, a number of different interpretations are possible. In Fig. 6, only one of them, which seems to be the most natural, is taken.

According to it, the first transition starts from the g.s. $9+[615]$ of the nucleus ^{271}Ds and leads to the low excited state $9+[615]$ of ^{267}Hs . This state decays by γ emission of the M1 type to the g.s. $7+[613]$. The second α -decay leads from this state to the low excited state $7+[613]$ of ^{263}Sg , which undergoes γ decay of the E2 type to a lower state $3+[622]$. From this state, the third α transition leads to a very low state $3+[622]$ of ^{259}Rf . We assume that this state decays by γ emission of the M1 type to the g.s. $1+[620]$, from which, the last α -transition leads to the g.s. state $1+[620]$ of ^{255}No .

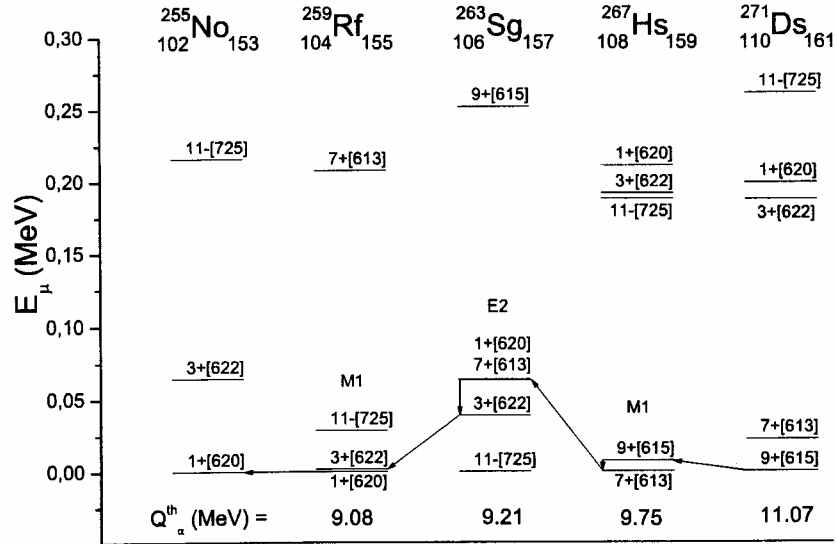


Fig. 6. Calculated single-particle spectra of nuclei belonging to the α -decay chain of the nucleus ^{271}Ds . Assumed sequence of consecutive α and γ decays is shown by the arrows. Type of the assumed γ decay (M1 or E2) for a given nucleus is shown. Theoretical values of α -decay energies Q_α of the nuclei are also given (at the bottom) [42].

Calculated and experimental values of α -transition energies Q_α^t along the described chain, as well as differences between them, $\delta Q_\alpha^t \equiv Q_\alpha^{t,\text{th}} - Q_\alpha^{t,\text{exp}}$, are given in the Table. Theoretical values of α -decay energies Q_α (g.s. to g.s. transitions) and the contribution ΔE of quasiparticle excitation energies to the α -transition energies Q_α^t , defined as

$$Q_\alpha^t \equiv Q_\alpha + (E_p - E_d) \equiv Q_\alpha + \Delta E, \quad (3)$$

is also given. Here, E_p and E_d are the excitation energies of the initial (parent nucleus) and final (daughter nucleus) states, respectively, between which the α transition occurs. Theoretical values of Q_α , Q_α^{th} , are taken from [32, 33]. Theoretical values of Q_α^t are calculated from Eq. (3) and experimental values of this quantity is taken from [33], where they were deduced from the data of [43, 44]. Alpha-decay half-lives T_α^{th} are calculated with the use of a simple 3-parameter phenomenological formula, proposed recently [45]. The formula reads

$$\log_{10} T_\alpha^{\text{ph}}(Z, N) = aZ[Q_\alpha^t(Z, N)]^{-1/2} + bZ + c, \quad (4)$$

where $Q_\alpha^t(Z, N)$ is the transition energy between initial (of the parent nucleus) and final (of the daughter nucleus) states of the α transition, Z and N are proton and neutron numbers of the parent nucleus, and $a = 1.5372$, $b = -0.1607$, $c = -36.573$.

The half-lives in Eq. (4) are in seconds and the transition energies Q_α^t are in MeV. The parameters a, b, c have been fitted to experimental values of T_α and Q_α for even-even nuclei with proton number $Z = 84 - 110$ and neutron number $N = 128 - 160$, for which both T_α [46] and Q_α [47] have been measured.

One can see in Eq. (4) that T_α is assumed to depend only, besides proton number Z , on the transition energy Q_α^t . As the same parameters a, b, c , adjusted to e-e (even-even) nuclei, are also used for o-e, e-o and o-o nuclei, no explicit hindrance factor is introduced (as it is done, e.g., in the Viola - Seaborg formula [48], which has been often used for a long time up to the present day (e.g., [29, 49 - 54])) for these nuclei. Thus, the decay of o-e, e-o and o-o nuclei is treated in the same way as e-e nuclei. The only difference is that nuclei with one or two odd nucleons do not usually decay from the ground state (g.s.) to the g.s., and this results in that the transition energy Q_α^t differs from the decay energy Q_α (corresponding to the g.s. to g.s. transitions). Only this difference is responsible for the variance between half-life of an o-e or e-o or o-o nucleus and an e-e one, in this description. This certainly concerns only the most probable (allowed) α decays of a nucleus, which decide about its half-life, in description of which we are interested here.

Values of characteristic quantities for the decay chain of ^{271}Ds (see text).

Nucleus	$Q_\alpha^{\text{t,th}}$	$Q_\alpha^{\text{t,exp}}$	$\delta Q_\alpha^{\text{t}}$	Q_α^{th}	ΔE	T_α^{th}	T_α^{exp}	f
-	MeV	MeV	MeV	MeV	MeV	-	-	-
^{271}Ds	11.06	10.91	0.15	11.07	-0.01	0.39 ms	1.1 ms	2.8
^{267}Hs	9.69	10.03	-0.34	9.75	-0.06	0.25 s	59 ms	4.2
^{263}Sg	9.25	9.39	-0.14	9.21	0.04	0.93 s	0.31 s	3.0
^{259}Rf	9.08	9.03	0.05	9.08	0.00	0.59 s	3.1 s	5.3

One can see in the Table that measured α -transition energies $Q_\alpha^{\text{t,exp}}$ are described with an average discrepancy $|\overline{\delta Q_\alpha^{\text{t}}}| = 0.17$ MeV. The discrepancy for all four decays does not exceed 0.34 MeV. The contribution of single-particle effects ΔE to Q_α^t is small, it does not exceed 0.06 MeV. The description of observed half-lives is also rather good. The ratio f of the larger value of T_α^{th} and T_α^{exp} to the smaller one does not exceed 5.3 and the average of this ratio for all four transitions is 3.8. One should stress that no free parameters have been used in the description of the discussed decay chain.

In conclusion, one can say the following:

1. Static fission barriers of superheavy nuclei are entirely created by effects of their shell structure. The largest shell effects are at the equilibrium point of a nucleus, but they are still significant at the saddle points.

Sufficiently large deformation space is important for the analysis of the barrier. Due to a faster decrease of the potential energy of a deformed nucleus at its equilibrium point than at the saddle one, with increasing dimension of the deformation space, the barrier height B_f^{st} increases when this dimension becomes larger.

Inclusion of non-axial shapes decreases B_f^{st} , as it decreases the energy at the saddle point, while not

changing it at the equilibrium point. This conclusion is also valid for a spherical (at equilibrium) heavy nucleus.

2. Concerning the single-particle properties of heaviest nuclei, the considered examples indicate that experimental single-particle excitation energies may be reproduced by the used macroscopic-microscopic model with an accuracy of about 200 keV. It is also indicated that the model allows to rather well describe transition energies and half-lives measured in observed α -decay chains.

The author would like to thank the coauthors of the reviewed articles for a fruitful cooperation. Support by the Polish State Committee for Scientific Research, grant no. 1 P03B 042 30, and the Polish-JINR (Dubna) Cooperation Programme is gratefully acknowledged.

REFERENCES

1. Hofmann S., Münzenberg G. // *Rev. Mod. Phys.* - 2000. - Vol. 72. - P. 733.
2. Oganessian Yu.Ts. et al. // *Nucl. Phys.* - 2001. - Vol. A 685. - P. 17c.
3. Armbruster P. // *Acta Phys. Pol.* - 2003. - Vol. B 34. - P. 1825.
4. Morita K. et al. // *Eur. Phys. J.* - 2004. - Vol. A 21. - P. 257.
5. Gregorich K.E. et al. // *Phys. Rev.* - 2005. - Vol. C 72. - P. 014605.
6. Möller P., Nix J.R. // *J. Phys.* - 1994. - Vol. G 20. - P. 1681.
7. Greiner W. // *Int. J. Mod. Phys.* - 1995. - Vol. E 5.
8. Sobczewski A. // *Usp. Fiz. Nauk.* - 1996. - Vol. 166. - P. 943; *Physics-Uspekhi.* - 1996. - Vol. 39. - P. 885.
9. Meng J., Toki H., Zhou S.G. et al. // *Prog. Part. Nucl. Phys.* - 2006 (in press).
10. Sobczewski A., Pomorski K. // *Prog. Part. Nucl. Phys.* - 2006 (in press).
11. Hoffman D.C., Lane M.R. // *Radiochim. Acta.* - 1995. - Vol. 70/71. - P. 135.
12. Gäggeler H.W. // *Proc. of the R.A. Welch Foundation 41st Conf. on Chemical Research: The Transactinide Elements.* - Houston: R.A. Welch Foundation, 1997. - P. 43.
13. Zvara I. // *Acta Phys. Pol.* - 2003. - Vol. B 34. - P. 1743.
14. Türler A. et al. // *Eur. Phys. J.* - 2003. - Vol. A 17. - P. 505.
15. Schädel M. // *Acta Phys. Pol.* - 2003. - Vol. B 34. - P. 1701.
16. *The Chemistry of Superheavy Elements* / Ed. M. Schädel. - Kluwer Acad. Publishers, 2003.
17. Armbruster P. // *Ann. Rev. Nucl. Part. Sci.* - 1985. - Vol. 35. - P. 135.
18. Smolańczuk R., Skalski J., Sobczewski A. // *Phys. Rev.* - 1995. - Vol. C 52. - P. 1871.
19. Świątecki W.J., Siwek-Wilczyńska K., Wilczyński J. // *Acta Phys. Pol.* - 2003. - Vol. B 34. - P. 2049.
20. Volkov V.V. // *Fiz. Element. Chastits i At. Yadra.* - 2004. - Vol. 35. - P. 797.
21. Itkis M.G., Oganessian Yu.Ts., Zagrebaev V.I. // *Phys. Rev.* - 2002. - Vol. C 65. - P. 044602.
22. Mamdouh A., Pearson J.M., Rayet M., Tondeur F. // *Nucl. Phys.* - 2001. - Vol. A 679. - P. 337.
23. Muntian I., Patyk Z., Sobczewski A. // *Acta Phys. Pol.* - 2003. - Vol. B 34. - P. 2141.
24. Möller P., Sierk A.J., Iwamoto A. // *Phys. Rev. Lett.* - 2004. - Vol. 92. - P. 072501.
25. Bürvenich T., Bender M., Maruhn J.A., Reinhard P.-G. // *Phys. Rev.* - 2004. - Vol. C 69. - P. 014307.
26. Krappe H.J., Nix J.R., Sierk A.J. // *Phys. Rev.* - 1979. - Vol. C 20. - P. 992.
27. Strutinski V.M. // *Nucl. Phys.* - 1967. - Vol. A 95. - P. 420; *Nucl. Phys.* - 1968. - Vol. A 122. - P. 1.
28. Ćwiok S., Dudek J., Nazarewicz W. et al. // *Comput. Phys. Commun.* - 1987. - Vol. 46. - P. 379.
29. Patyk Z., Sobczewski A. // *Nucl. Phys.* - 1991. - Vol. A 533. - P. 132.
30. Muntian I., Patyk Z., Sobczewski A. // *Acta Phys. Pol.* - 2001. - Vol. B 32. - P. 691.
31. Audi G., Bersillon O., Blachot J., Wapstra A.H. // *Nucl. Phys.* - 1997. - Vol. A 624. - P. 1.
32. Muntian I., Patyk Z., Sobczewski A. // *Yad. Fiz.* - 2003. - Vol. 66. - P. 1051; *Phys. At. Nucl.* - 2003. - Vol. 66. - P. 1015.
33. Muntian I., Hofmann S., Patyk Z., Sobczewski A. // *Acta Phys. Pol.* - 2003. - Vol. B 34. - P. 2073.
34. Sobczewski A., Muntian I. // *Nucl. Phys.* - 2004. - Vol. A 734. - P. 176.
35. Sobczewski A., Muntian I. // *Int. J. Mod. Phys.* - 2005. - Vol. E 14. - P. 409.
36. Muntian I., Sobczewski A. // *Int. J. Mod. Phys.* - 2005. - Vol. E 14. - P. 417.
37. Sobczewski A., Kowal M. // *Phys. Scr.* - 2006. - Vol. T 125 (in press).
38. Bjornholm S., Lynn J.E. // *Rev. Mod. Phys.* - 1980. - Vol. 52. - P. 725.
39. Muntian I., Sobczewski A. // *Acta Phys. Pol.* - 2005. - Vol. B 36. - P. 1359.
40. Parkhomenko O., Sobczewski A. // *Acta Phys. Pol.* - 2004. - Vol. B 35. - P. 2447.
41. Parkhomenko A., Sobczewski A. // *Int. J. Mod. Phys.* - 2005. - Vol. E 14. - P. 421.
42. Parkhomenko A., Sobczewski A. // *Int. J. Mod. Phys.* - 2006. - Vol. E 15. - P. 457.
43. Hofmann S. // *Rep. Prog. Phys.* - 1998. - Vol. 61. - P. 639.
44. Hofmann S. // *Acta Phys. Pol.* - 1999. - Vol. B 30. - P. 621.
45. Parkhomenko A., Sobczewski A. // *Acta Phys. Pol.* - 2005. - Vol. B 36. - P. 3095.
46. Audi G., Bersillon O., Blachot J., Wapstra A.H. // *Nucl. Phys.* - 2003. - Vol. A 729. - P. 3.

47. *Wapstra A.H., Audi G., Thibault C.* // Nucl. Phys. - 2003. - Vol. A 729. - P. 129.
48. *Viola V.E. Jr., Seaborg G.T., Inorg J.* // Nucl. Chem. - 1966. - Vol. 28. - P. 741.
49. *Böning K., Patyk Z., Sobiczewski A., Ćwiok S.* // Z. Phys. - 1986. - Vol. A 325. - P. 479.
50. *Sobiczewski A., Patyk Z., Ćwiok S.* // Phys. Lett. - 1989. - Vol. B 224. - P. 1.
51. *Lalazissis G.A., Sharma M.M., Ring P., Gambhir Y.K.* // Nucl. Phys. - 1996. - Vol. A 608. - P. 202.
52. *Łojewski Z., Baran A.* // Z. Phys. - 1988. - Vol. A 329. - P. 161.
53. *Gambhir Y. K., Bhagwat A., Gupta M., Jain A.K.* // Phys. Rev. - 2003. - Vol. C 68. - P. 044316.
54. *Zhang W., Meng J., Zhang S.Q. et al.* // Nucl. Phys. - 2005. - Vol. A 753. - P. 106.

СВОЙСТВА ТЯЖЕЛЫХ И СВЕРХТЯЖЕЛЫХ ЯДЕР

А. Собичевский

Кратко рассмотрены последние исследования свойств самых тяжелых ядер, выполненные нашей теоретической группой в Варшаве. Исследования концентрируются главным образом на двух темах: высотах статических барьеров деления B_f^{st} и одночастичных свойствах таких ядер. При анализе B_f^{st} решающую роль играет пространство деформаций, используемое при анализе. Показаны результаты, полученные в случае, когда разрешены только аксиально-симметричные формы, а также, когда включаются неаксиальные деформации. Обсуждаются одноквaziчастичные спектры самых тяжелых ядер. Иллюстрируется влияние одноквaziчастичных спектров на переходные энергии цепочек α -распадов и на периоды α -распадов.

ВЛАСТИВОСТІ ВАЖКИХ ТА НАДВАЖКИХ ЯДЕР

А. Собічевський

Коротко оглянуто останні дослідження властивостей найважчих ядер, що виконано нашою теоретичною групою у Варшаві. Дослідження концентруються головним чином на двох темах: висотах статичних бар'єрів розщеплення B_f^{st} і одночастинкових властивостях таких ядер. При аналізі B_f^{st} вирішальну роль відіграє простір деформацій, що використовується при аналізі. Показні результати, одержані у випадку, коли дозволяються лише аксиально-симетричні форми, а також, коли включаються неаксиальні деформації. Обговорюються одноквzичастинкові спектри найважчих ядер. Проілюстровано вплив одноквzичастинкових спектрів на перехідні енергії ланцюжків α -розпадів і на періоди α -розпадів.